Global Ecology and Biogeography, (Global Ecol. Biogeogr.) (2006) **15**, 553–566

RESEARCH PAPER

Simulated ecosystem threshold responses to co-varying temperature, precipitation and atmospheric CO_2 within a region of Amazonia

Sharon A. Cowling* and Younglan Shin

Department of Geography, University of Toronto, 100 St. George Street, Toronto, Ontario, M5S 3G3, Canada

ABSTRACT

Aim Using a Dynamic Global Vegetation Model (DGVM), we assessed the independent and co-varying effects of temperature, precipitation and atmospheric CO_2 on nonlinear (threshold) responses in carbon-based processes, and evaluated whether these underlying process thresholds translate to the ecosystem-scale.

Location Amazon Basin, South America.

Methods The Lund-Potsdam-Jena model (LPJ) was employed to determine responses in net primary production (NPP), heterotrophic respiration (R_H), vegetation carbon (C_V), soil carbon (C_S), and plant functional type (PFT) composition to variations in temperature (± 9 °C relative to the control), precipitation (up to 80% reduction in rainfall relative to the control) and atmospheric CO_2 (± 100 p.p.m.v. relative to the control).

Results Our modelling experiments show that increases in temperature result in lower and steeper NPP and R_H curves, indicating a thermal threshold at current temperature conditions. Under a combination of temperature and precipitation change, C_V responds more to precipitation, while C_S closely follows temperature gradients. Ecosystem thresholds, measured in terms of PFT composition stability, are surprisingly few. Simulations indicate an ecosystem threshold occurring at 80% reduction in rainfall; however, due to modelling limitations, this threshold is likely to occur at earlier drought stress conditions. Further empirical research on abiotic stress tolerance levels in tropical ecosystems must be performed in order to refine PFT descriptions used in DGVMs.

Main conclusion In evaluating simulation scenarios that promote major changes in PFT assemblage, we conclude that the 'natural' Amazonian rain forest is resilient to environmental change, particularly to decreases in temperature and precipitation. Determining to what extent anthropogenic pressures have altered this resiliency is of utmost importance in predicting the future fate of the Amazon Basin.

*Correspondence: Sharon A. Cowling, Department of Geography, University of Toronto, 100 St. George Street, Toronto, Ontario, M5S 3G3, Canada.
E-mail: cowling@geog.utoronto.ca

Keywords
Amazon, atmospheric CO_2 change, carbon storage, climate change, dynamic global vegetation model, ecological thresholds, LPJ, plant functional types, tropical forests.

INTRODUCTION

Processes and mechanisms affecting carbon dynamics and vegetation structure in undisturbed tropical forests are highly sensitive to changes in climate and atmospheric CO_2 (Post *et al.*, 1997). A common theme in global change research is the presence of nonlinear responses of ecophysiological and biochemical processes to environmental change (Mayer & Rietkerk, 2004). Often, nonlinear processes yield 'threshold'-like response curves, indicating that a process is resilient to change up to a specific point, after which further change causes a sharp response, either a rapid increase or decrease relative to pre-threshold values. Understanding the limits of processes in resisting change is necessary if we are to make accurate predictions

© 2006 The Authors
Journal compilation © 2006 Blackwell Publishing Ltd
DOI: 10.1111/j.1466-822x.2006.00256.x
www.blackwellpublishing.com/geb

of how ecosystem-level processes may become altered in the near future.

Not only have thresholds been associated with physiological and biochemical terrestrial processes, but they have also been discussed in the context of ecosystem-scale processes and functions (Eiswerth & Haney, 2001; Reynolds, 2002; Stringham *et al.*, 2003). Much has been written about 'ecosystem resilience' in the literature, with two definitions of resiliency having become most popular. Ecosystem resiliency is either viewed from the perspective of an ecosystem overcoming catalysts promoting change, or of an ecosystem that is disturbed and is able to return to its pre-disturbed state (Peterson *et al.*, 1998). Studies have been carried out, for example, to determine whether there are threshold relationships between degrees of deforestation and bird abundance and richness in various forested landscapes (Lindenmayer *et al.*, 2005; Radford *et al.*, 2005), and between aphid populations and the degree of forest fragmentation (With *et al.*, 2002).

Threshold responses can occur simply from the change in one single environmental factor, or can be the result of combined effects from multiple environmental factors. Separating the effects of the two can be difficult in field or laboratory experiments, however, the use of models can be of particular importance in this respect (House *et al.*, 2003). Vegetation model simulations can reveal potential nonlinear, threshold responses, and can do so at the level of individual processes (i.e. photosynthesis) and at the community (ecosystem) level (based on competition between various plant functional types, PFTs).

The objective of our research incorporating the use of a dynamic vegetation model was three-fold. First, we wanted to identify which of the commonly cited carbon-based variables (i.e. NPP, R_H, C_V and C_S) show the strongest threshold effects in response to changes in temperature, precipitation and atmospheric CO_2. Secondly, we wanted to determine if these threshold effects arise from one environmental stimulus acting independently, or to two or more stimuli acting in combination. Lastly, we were interested in determining whether threshold effects could be seen at the community (ecosystem) level, and whether our modelled Amazonian system showed signs of resiliency to environmental change. For this analysis, we considered changes in the relative abundance and composition of regional PFTs.

We chose to model a small region within the Amazonian watershed (area enclosed by 3° N–8° S and 63° W–73° W), based on the rationale that a smaller area is likely to show more homogeneous responses than a larger area (Alcock, 2003). The influence of nutrient limitations (Chambers & Silver, 2004a) and other natural and anthropogenic disturbances (i.e. deforestation, forest re-growth and biomass burning) (Garcia-Romero *et al.*, 2004; Larsen *et al.*, 2005) are inarguably important when considering tropical forest thresholds, however, they are beyond the scope of this current study.

METHODS

Model description

The Lund-Potsdam-Jena (LPJ) Dynamic Global Vegetation Model (DGVM) (Sitch *et al.*, 2003) simulates dynamic responses in carbon processes, vegetation structure, and soil biogeochemistry. Vegetation structure is defined by 10 PFTs and is based on physiological (C_3, C_4), phenological (deciduous, evergreen) and physiognomic (tree, grass) attributes. Each PFT can occur as a fraction of a grid depending on the bioclimatic limits of each PFT. These limits are based on 20-year running means (Table 1). Each PFT population is characterized by a set of variables describing the state of the average individual, as well as by the population density. More detailed parameter values for each PFT can be found in Sitch *et al.* (2003) and Haxeltine & Prentice (1996).

Competition for light and water are modelled via PFT-specific attributes. Photosynthesis is modelled following a simplified Farquhar approach, with the carbon and water cycles coupled through the calculation of canopy conductance. Annual NPP is allocated to leaf, sapwood, and fine root carbon pools, satisfying a prescribed set of structural constraints. Plant respiration is simulated in response to both temperature and moisture limitations.

A two-layer soil module is incorporated in LPJ and is based on parameterizations developed in BIOME3 (Haxeltine & Prentice, 1996). The water content in each layer is determined mostly by soil texture, including soil properties such as water holding capacity. Each PFT has an associated above- and below-ground litter pool. As litter decomposes, 70% of the carbon goes directly

Table 1 Selected parameterizations used to define plant functional types (PFTs) incorporated in the vegetation model, LPJ. P_n refers to photosynthetic pathway (C_3 or C_4). W refers to a water stress threshold scalar used to calculate maximum leaf coverage. T_{low} is low temperature limit for CO_2 uptake (photosynthesis). T_1 and T_2 are the lower and upper range of photosynthetic temperature optima, respectively. T_{max} is the high temperature limitation for CO_2 uptake

PFT	P_n	W	T_{low}	T_1 (°C)	T_2 (°C)	T_{max} (°C)
Tropical broad-leaved evergreen	C_3	0.0	2.0	25.0	30.0	55.0
Tropical broad-leaved raingreen	C_3	0.35	2.0	25.0	30.0	55.0
Temperate needle-leaved evergreen	C_3	0.0	−4.0	20.0	30.0	42.0
Temperate broad-leaved evergreen	C_3	0.0	−4.0	20.0	30.0	42.0
Temperate broad-leaved summergreen	C_3	0.0	−4.0	20.0	25.0	38.0
C_3 grass	C_3	0.35	−4.0	10.0	30.0	45.0
C_4 grass	C_4	0.35	6.0	20.0	45.0	55.0

© 2006 The Authors

into the atmosphere, and the remaining 30% is divided into the intermediate-turnover (98–98.5%) and slow-turnover (1.5%) soil pools. The decomposition rate of litter and soil is both temperature and moisture dependent.

LPJ includes a fire module that simulates the release of CO_2 from the biosphere to the atmosphere. The role that fire plays in the terrestrial carbon budget is dependent on: (1) fuel availability, (2) litter moisture, (3) length of the fire season, and (4) PFT-specific fire tolerances. LPJ incorporates all four considerations.

Validation of the ability of LPJ to realistically simulate process variables has been undertaken by many modelling groups (Gordon *et al.*, 2004; Peylin *et al.*, 2005; Sitch *et al.*, 2005). Consequently, LPJ is used extensively in both global and regional simulations, and can be used for research questions related to the response of terrestrial ecosystems to seasonal and inter-annual climate variability (Dargaville *et al.*, 2002; Lucht *et al.*, 2002; Sitch *et al.*, 2003; Gerber *et al.*, 2004). In addition, LPJ has also proved a useful tool for palaeovegetation research (Kaplan *et al.*, 2002; Joos *et al.*, 2004).

Simulated region

We simulated a region of the Amazon Basin, South America, described by an area enclosed by co-ordinates 3° N to 8° S and 63° W to 73° W. Our region is characterized by a mean monthly temperature and precipitation rate of 24.3 °C and 202 mm, respectively. These numbers represent an average taken over the entire time sequence, 1901–98. This area is comparable to about 20% of the entire Amazonian watershed. Tropical broadleaf evergreen forest is the dominant biome type in the region (Ramankutty & Foley, 1999). As with tropical regions in general, carbon in our simulations is mostly stored in above-ground relative to below-ground pools (Townsend & Vitousek, 1992).

Input data

Input parameters, measured at a resolution of 0.5° by 0.5° latitude/longitude, include: (1) soil type, (2) monthly temperature, (3) monthly precipitation, (4) cloud cover (that in turn is converted into percentage sunshine), and (5) annual atmospheric CO_2 concentration. Soil type was derived from Zobler's modified soil data base (Post & Zobler, 2000). Our control atmospheric CO_2 data base was obtained from the Carbon Cycle Model Linkage Project, and includes measurements and/or extrapolations from the years 1901 to 1998 (Kicklighter *et al.*, 1999; McGuire *et al.*, 2001).

Monthly climate data used in our study (New *et al.*, 2003) is the most comprehensive observational data base available today, and covers the period from 1901 to 1998. These data are constructed using an anomaly approach, measured relative to a normalized time sequence between the years 1961–90. The climate anomaly approach represents a large step forward in global change research as climatology is no longer biased by the General Circulation Models (GCMs) in which the data base was generated. Anomaly grids were combined with a high-resolution mean monthly climatology to produce modelling input data. The Amazon region in particular has few climate monitoring stations (New *et al.*, 2000), thus climatological interpolation may have introduced some error in our simulations; however, this is likely not to be significant enough to alter overall trends.

Modelling scenarios

Control simulation

Because LPJ simulates terrestrial ecosystems from bare ground, a minimum of 1000 years of simulation is required to accurately represent carbon in soil, vegetation and litter pools. We conducted our 1000-year spin-up simulation by using climate data from the early portion of the modern-day data set (i.e. 1901–20) and by employing constant preindustrial atmospheric CO_2 levels of 280 p.p.m.v. Post-spin-up, our control simulation incorporated the full 1901–98 climate data base, and included atmospheric CO_2 that varied from a minimum concentration of 296 p.p.m.v. to a maximum concentration of 365 p.p.m.v..

Experimental simulations

Our experimental simulations involved applying each climate anomaly independently and in combination with other climate and CO_2 anomalies. To evaluate the independent influence of temperature and precipitation, we conducted simulations using temperature increases of 3, 5, 7 and 9 °C, temperature decreases of 3, 5, 7 and 9 °C and precipitation reductions of 20, 40, 60 and 80% relative to the control. To evaluate their combined effects, we conducted a total of 45 simulations (including all possible crosses of the climate anomalies indicated, and our control simulation). Although scenarios involving increases in precipitation might have generated interesting results, we did not consider this aspect based on the assumption that precipitation is not a limiting factor in humid tropical forests. We also did not consider percentage cloud cover anomalies, since the effects of changes in cloud cover on carbon dynamics are relatively small (Gerber *et al.*, 2004). To examine the influence of atmospheric CO_2 on combined temperature (± 5 and ± 7 °C) and precipitation (40% and 80% rainfall reduction), we simply prescribed atmospheric CO_2 levels of +100 p.p.m.v. and −100 p.p.m.v. relative to the control CO_2, generating an additional 30 simulations.

MODEL VALIDATION

Comparison with other modelling studies

All simulation results are reported as averages calculated over the entire modelled region, because our main objective did not involve evaluating landscape heterogeneity. We were also not concerned with inter-annual variability *per se* therefore comparisons were made based on the equilibrium response at the final year of simulation. Our comparative analyses are focused on the following diagnostic variables: NPP, R_H, net ecosystem productivity (NEP), C_V and C_S.

© 2006 The Authors

NPP for our control simulation was 968 g C m^{-2} $year^{-1}$. Potter *et al.* (2001) estimate that mean NPP for the Brazilian region of the Amazon watershed is between a lower end of 780–1030 g C m^{-2} $year^{-1}$ to an upper end of 950–1300 g C m^{-2} $year^{-1}$. Similarly, NPP simulated for the entire Amazon Basin by Cramer *et al.* (2004) yields a value of 981 g C m^{-2} $year^{-1}$.

We simulated an average R_H value of 867 g C m^{-2} $year^{-1}$, similar to Cramer *et al.*'s (2004) simulation of 931 g C m^{-2} $year^{-1}$. Including root respiration, Raich *et al.* (2002) estimated Amazonian R_H to be around 1320 g C m^{-2} $year^{-1}$, calculated for the years between 1980 and 1994. Their observations were taken from an evergreen broadleaf forest growing under a climate regime characterized by a mean temperature of 24.6 °C and a mean annual precipitation of 2214 mm. Assuming that about 30–40% of total respiration is from root biomass, our simulated R_H value is within the same range as that of Raich *et al.* (2002).

Carbon dioxide flux caused from the burning of terrestrial carbon is simulated to be 30 g C m^{-2} $year^{-1}$. Our simulated NEP was roughly 71 g C m^{-2} $year^{-1}$, consistent with Chambers *et al.*'s (2004b) estimate of an Amazonian carbon sink of close to 50 g C m^{-2} $year^{-1}$. During El Niño years, Potter *et al.* (2001) simulate an Amazonian carbon source in excess of 100 g C m^{-2} $year^{-1}$, and simulate a carbon sink of 50–200 g C m^{-2} $year^{-1}$ in other years. Kucharik *et al.*'s (2000) modelling research indicates that between 37 and 53 g C m^{-2} $year^{-1}$ was accumulated in tropical forests during the period of 1965–94.

Our final year simulation of C_V (7 kg C m^{-2}) is on the lower end of ranges reported by other modelling studies conducted in similar areas of South America. For the entire Amazon watershed, Sitch *et al.* (2003) model average C_V in the range of 15–18 kg C m^{-2}. For the Amazon, defined by an area enclosed by 3° N to 8° S and 63° W to 73° W, Cox *et al.* (2004) estimate C_V equal to approximately 12.4 kg C m^{-2}. We suggest two possible explanations for our C_V values falling on the lower-end estimates relative to other modelling research: (1) our simulated site contains mixed PFTs, thus carbon uptake by other PFTs is generally lower than for tropical broadleaf evergreen forest itself, and therefore would contribute to an overall lower net productivity regionally, and (2) we simulated a very small portion of the Amazon watershed which may not entirely be representative of the basin as a whole. Subsequent modelling experiments indicated that when LPJ was simulated for 200 years (as opposed to 98 years), C_V values were in fact higher (data not shown), and more similar to other modelled values (i.e. Tian *et al.*, 2000).

With respect to C_S, our simulated values are consistent with other modelling studies. C_S is simulated at 4.1 kg C m^{-2}, while Sitch *et al.* (2003) predict C_S in the range of 3–6 kg C m^{-2}, and Cox *et al.* (2004) estimate C_S to be 5 kg C m^{-2}. Simulated litter carbon (C_L) for our region of Amazonia (0.6 kg C m^{-2}) falls within the range estimated for tropical forests in general (0.4–0.6 kg C m^{-2}) (Kucharik *et al.*, 2000).

Comparison with observational data

A direct comparison of our simulated values to those observed cannot be made due to the lack of field data undertaken within our simulated region (as well as across Amazonia in general). We have, however, provided a range of observational values gathered at various places throughout Amazonia and within the humid tropics (Table 2) to aid in qualitative comparisons. Our control NPP is indirectly compared against above-ground coarse woody carbon production (which is approximately proportional to total above-ground productivity) measured in 104 plots within Amazonian humid tropical forest (Malhi *et al.*, 2004). Malhi *et al.* (2004) show that most plots in lowland central and eastern Amazonia have a relatively low productivity, with the highest productivities occurring in western Amazonia. Malhi *et al.* (2004) observed an upper limit of above-ground NPP of around 1260 g C m^{-2} $year^{-1}$. We chose values of above-ground coarse woody carbon production for six of Malhi *et al.*'s (2004) sites and calculated NPP (by multiplying by 2.93) to obtain a relative range of NPP values. Chosen sites were taken from areas characterized by rainfall rates of 2272–2763 mm $year^{-1}$ and mean temperatures of between 25 and 27 °C (i.e. similar to our modelled region). Observed above-ground NPP ranged from 747 to 957 g C m^{-2} $year^{-1}$, in contrast to our simulated NPP value of 968 g C m^{-2} $year^{-1}$. Our simulated value, however, included below-ground root biomass.

Table 2 Comparison between simulated and observed annual carbon fluxes (g C m^{-2} $year^{-1}$), including net primary production (NPP), heterotrophic respiration (R_H), net ecosystem production (NEP), and carbon storages (Kg C m^{-2})

	Simulated	Field sudy	Region or biome type
NPP	968	747–957	Amazon
R_H	867	890–1520	Moist humid forest
NEP	71	62	Amazon
C_V	7	4–25	Tropical broad-leaved humid forest
C_S	4	3.5–10.9	Amazon

For R_H comparisons, we chose observational soil respiration flux data for a tropical moist/humid forest region defined by rainfall rates greater than 1500 mm $year^{-1}$ (i.e. once again to be consistent with our modelled region). Values of R_H observed by Raich & Schlesinger (1992) and Silver (1998) fall between 890 and 1520 g C m^{-2} $year^{-1}$. Assuming that root respiration contributes approximately 30% to total soil respiration, our value of R_H is in good agreement with observational data (Table 2). Similarly, net carbon uptake rates of 62 ± 37 g C m^{-2} $year^{-1}$ obtained in the field (Amazonia) by Phillips *et al.* (1998) are comparable to our simulated NEP rate. Eddy flux NEP measurements reported for tropical forests can vary substantially, for example, between 70 and 590 g C m^{-2} $year^{-1}$ (Prentice *et al.*, 2001). Our simulated value of C_V falls within the lower end of reported field-based ranges (4–25 kg C m^{-2}) (Olson *et al.*, 2003). Simulated C_S was in good agreement with data extracted from soil surveys taken in a region in the Amazon (0.1° N by 68.4° W) between the years 1965–84 (Zinke *et al.*, 2003).

Simulated PFT fractions are compared with extracted vegetation types generated from satellite surveys (DeFries *et al.*, 1999;

© 2006 The Authors

Table 3 Comparison between observed and simulated PFT fractional coverage (%)

PFT	Observation	Simulated
Broadleaf tree	80.1 ± 8.7	86.2 ± 9.3 (total broad-leaved)
		72.8 ± 17.9 (tropical PFT only)
Evergreen tree	77.5 ± 9.6	64.0 ± 10.6 (total evergreen)
		48.5 ± 14.4 (tropical PFT only)
Deciduous tree	2.6 ± 3.4	29.5 ± 9.8 (total deciduous)
		23.7 ± 12.0 (tropical PFT only)
Tree	80.1 ± 8.7	93.6 ± 5.5 (total tree)
Grass	17.9 ± 8.3	6.0 ± 5.5 (total grass)

DeFries *et al.*, 2000). Cover type distributions were derived from multi-temporal Advanced Very High Resolution Radiometer (AVHRR) data and were originally mapped at 1-km resolution, then later aggregated at the 0.5° × 0.5° latitude/longitude scale. The number of vegetation types (i.e. PFTs) is far fewer in the satellite data base relative to LPJ, therefore there were several ways in which we could aggregate our simulated PFTs to compare against those from the observational data base (leading to either overlapping data or absent data). For example, satellite classification of 'broadleaf trees' is represented by three PFTs in LPJ: broadleaf evergreen, broadleaf deciduous and temperate broadleaf. We present, therefore, two simulation results for each vegetation type: one in which all possibilities are considered resulting in an overestimation of fractional coverage, and the other in which just one humid tropical PFT is considered, resulting in an overall underestimation of fractional coverage (Table 3).

Our simulated broadleaf cover is well captured under both comparison methods, as is our simulated evergreen tree PFT (Table 3). Thus, we are confident that LPJ is simulating realistic percentage cover values for tropical rainforest within our selected region. Simulations of deciduous trees are overestimated in LPJ relative to satellite data (Table 3). Satellite data indicate that less than 3% of our modelled region contains deciduous tree cover, whereas LPJ simulates between 24% and 30% of the area covered with broadleaf raingreen (seasonal) forest. This implies that LPJ is limited in its abilities to distinguish between a humid and seasonal tropical forest. A limitation such as this indicates that the stress tolerance levels (input parameters) assigned to each of the competing PFTs must be reviewed and refined, not only in LPJ but also in other first-generation global vegetation models.

Compared to DeFries *et al.*'s (1999) satellite-based vegetation distributions, LPJ overestimates the amount of tree cover and subsequently underestimates the amount of grass cover in Amazonia. This trend has also been reported in other DGVM model simulations of the Amazon Basin (Cox *et al.*, 2004). Many factors influence competition between grass and woody perennials, including primarily fire, but also including anthropogenic land-use change, which is generally omitted or is only crudely parameterized in vegetation models. Overall, however, we feel that LPJ simulations of vegetation cover in our region of Amazonia are robust enough to place good confidence in the results we obtain during our sensitivity-type modelling experiments.

RESULTS AND DISCUSSION

Process thresholds: NPP, R_H and carbon storage

Simulated NPP and R_H are relatively insensitive to temperature cooling (i.e. temperature anomalies up to −9 °C relative to the control) (Fig. 1a). NPP, for example, varies by less than 2% over the full range of cooling. In contrast, NPP and R_H decrease in total by 28% and 26%, respectively, when temperatures increase from the control to +9 °C. The adverse effects of temperature warming on tropical forest NPP are consistent with other modelling studies (Botta *et al.*, 2002; Gerber *et al.*, 2004; Potter *et al.*, 2004) and field measurements (Malhi *et al.*, 2004). If we define 'threshold' as a point in time when there occurs a sharp change in response to external stimuli, then modelling results indicate that NPP has a temperature threshold hovering near modern-day values.

Under independent temperature changes, R_H is relatively insensitive to cooling scenarios, much like NPP (Fig. 1a). Field studies indicate a close correlation between NPP & R_H in various ecosystems (Raich & Schlesinger, 1992). R_H and NPP both decline with increasing temperature, although the slope of the decline in R_H is somewhat less steep than that of NPP. Even though increasing temperature should increase rates of decomposition, R_H declines with increasing temperatures due to the overriding effect of reduced litter input resulting from low vegetation productivity (Potter *et al.*, 2004). Simulated R_H also shows a threshold around modern-day temperatures.

Modelling simulations performed with combined temperature and precipitation anomalies indicate that the interaction of these two climate variables does not result in a sharpening of thresholds (i.e. increase downward slope), but actually results in a smoothening of the slope of both NPP and R_H response curves (Fig. 1b,c). By the time precipitation is decreased by 80% relative to the control, our NPP vs. temperature curve is close to linear, with cooler temperatures resulting in the highest NPP when combined with severe water stress.

Similarly, the smoothening of the threshold curve in response to decreased precipitation also occurs with R_H, although our extreme drought scenario results in a complete lack of response of R_H with any change in temperature, either warming or cooling (Fig. 1c). Field observations of the co-varying effects of inter-annual changes in soil water content (SWC) and temperature within a temperate pine forest indicate that when SWC is less than 15%, the rate of R_H declines and is insensitive to changes in air (soil) temperatures (Yuste *et al.*, 2003).

Reduction in both NPP and R_H with increasing temperature is only minimally enhanced in combination with low precipitation. In our modelled region of Amazonia, a reduction in precipitation by up to 60% relative to that today has generally minimal effect on NPP and R_H. The largest decrease in NPP occurs with a reduction of precipitation by 80%. We believe that our simulated NPP threshold (at 80% reduction in rainfall relative to the control) is

© 2006 The Authors

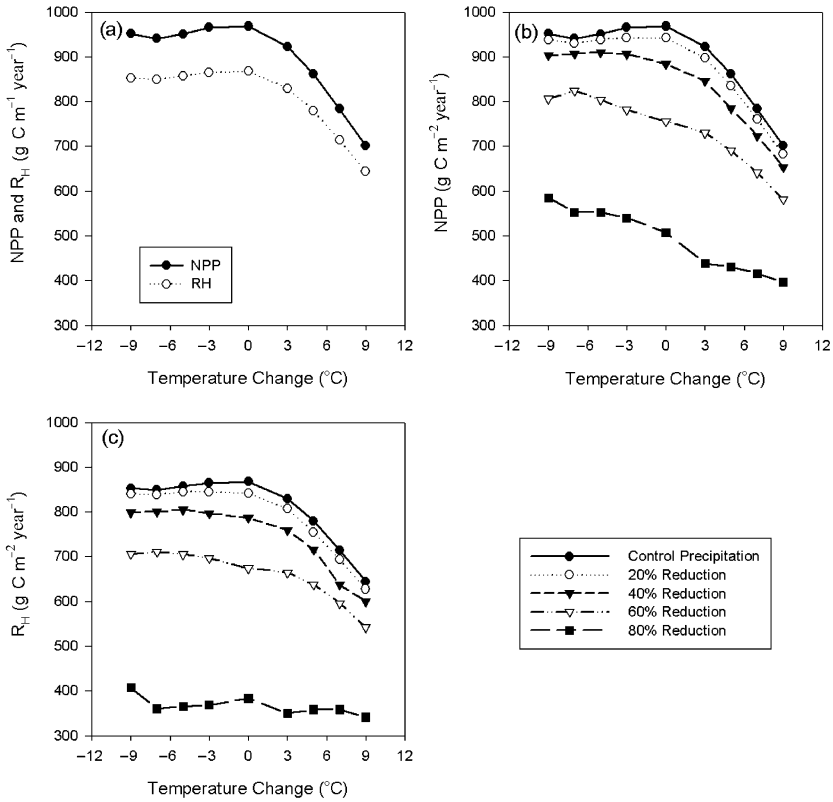

Figure 1 Response of (a) net primary production (NPP) and heterotrophic respiration (R_H) to variations in temperature, (b) NPP under combined temperature and precipitation change, and (c) R_H under co-varying temperature and precipitation stress.

unrealistic. In reality, precipitation thresholds in tropical humid forests are likely to occur at less water-stressed conditions than our modelled 80% reduction threshold. Two reasons may account for an underestimation of the response of tropical forest to water stress. First, the water stress threshold scalar (see Table 1) may not be robust enough to capture realistic responses of tropical forest to drought. The use of PFTs in vegetation models was initially a necessity because of computational constraints; however, with the growing amount of useful ecophysiological data, modelled PFT tolerances can soon be refined, overcoming this constraint. Secondly, LPJ is unable to accommodate vegetation–climate feedbacks on regional rainfall. The Amazon Basin is characterized by a high recycling rate of precipitation (Marengo *et al.*, 1994), thus even small changes in vegetation abundance or NPP in response to decreases in precipitation will cause a positive feedback on localized drying (Betts *et al.*, 2004). Recent modelling research on the effects of future climate change on the Amazon Basin indicates that initial decreases in percentage forest cover promoted by sea surface warming and reduced precipitation result in less evaporative recycling of rainfall and enhanced local surface temperatures (see scenario IS92a in Cox *et al.*, 2004).

On the other hand, other studies indicate that rainfall over forest vegetation appears to be almost insensitive to soil water stress, whereas reduced precipitation is generated only over pasture-dominated landscapes (da Rocha *et al.*, 1996). This study indicates a strong resilience in highly forested regions to a disturbance in the vegetation-rainfall recycling process; thus our estimate of a threshold of around 80% decrease in precipitation may be less unrealistic than at first glance.

According to Foley *et al.* (2002), precipitation change associated with ENSO years is roughly 20% below rainfall characteristic of 'neutral' years, with temperature changes arising from ENSO considered fairly small, in the order of 0.3 °C warming. Based on our co-varying climate simulations, such a combination of environmental stresses should have minimal influence on net productivity, however, other modelling and field observations suggest otherwise (Tian *et al.*, 2000). This discrepancy can be explained by the fact that LPJ does not model anthropogenic changes in fire frequency, whereas in reality, the interaction of ENSO climate and fire (promoted by clear-cutting, selective cutting and burning of pasture fields) results in a substantial reduction in Amazonian productivity (Laurance & Williamson, 2001; Laurance, 2003; Barlow & Peres, 2004), heightening Amazonia's sensitivity to fire disturbance. Normally in humid tropical forests, precipitation is not a limiting factor to ecosystem productivity, whereas in tropical savanna regions, a reduction in precipitation is usually the most prominent factor promoting active competition between grass and tree types (via fire interactions) (Smith *et al.*, 2001; Botta *et al.*, 2002).

Carbon stored in vegetation (C_V), soil (C_S) and litter (C_L) differ slightly in their response to co-varying temperature and precipitation climate stress (Fig. 2). C_V responds less variably under temperature cooling scenarios, but shows a steeper response under temperature warming. Overall, changes in precipitation have more of an effect on C_V than on C_S (Fig. 2a,b). C_S displays almost a linear trend when temperature changes are combined with rainfall reductions of up to 60%. C_L responds in a similar manner as C_S (Fig. 2c), showing minimal sensitivity to changes in precipitation, even under an

© 2006 The Authors

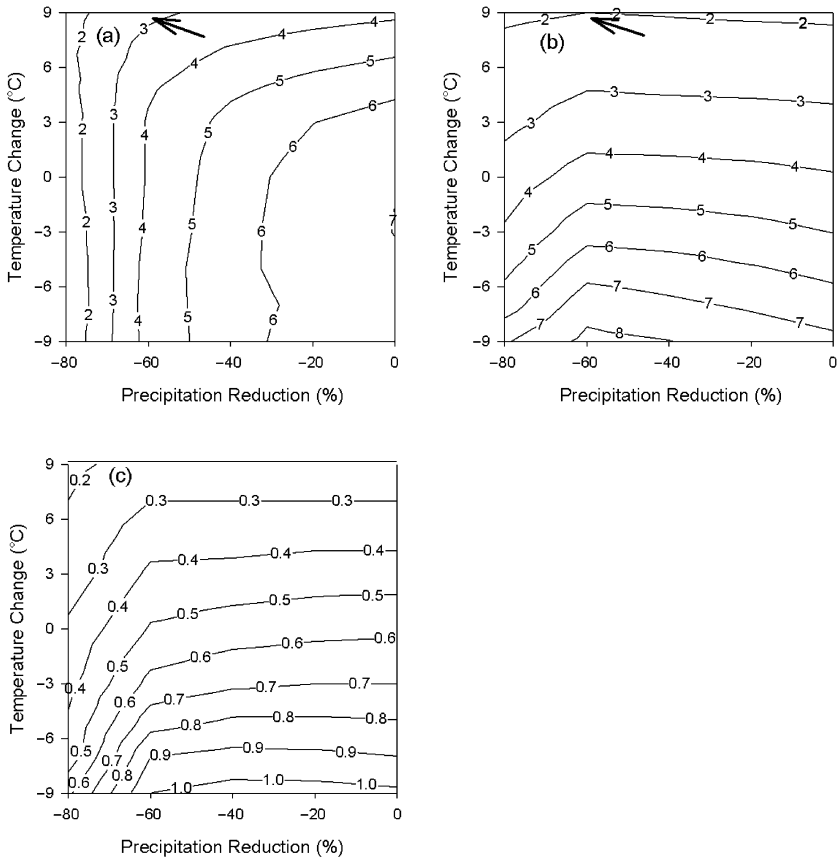

Figure 2 Effects of co-varying temperature and precipitation stress on (a) vegetation carbon (C_V), (b) soil carbon (C_S), and (c) litter carbon (C_L). Unit of carbon storage is kg C m^{-2}. Arrows indicate projected regional climate change to occur by the year 2090, as generated from HadCM3LC simulations under the IS92a CO_2 emission scenario (Cox *et al.*, 2004).

80% reduction in precipitation. Our co-varying climate anomaly simulations clearly show the dependence of C_S and C_L on ambient temperature. Both trends can be accounted for by their strong sensitivity of decomposition rate to temperature fluctuations (Gerber *et al.*, 2004).

General trends derived from our simulations using a DGVM can be useful in providing further insight into climate change research performed at the scale of (coupled) GCMs. If lower resolution models (like LPJ) can predict the relative change in carbon variables like C_V and C_S to future changes in climate that are similar to the responses indicated by GCMs, then greater confidence can be placed on these future predictions. TRIFFID, for example, simulates a future (end of the 21st century) decrease in Amazonian C_V and C_S by 22% and 28%, respectively, in response to a warming of 9.2 °C and a decrease in rainfall by 36% (Cox *et al.*, 2004). TRIFFID is a component of the Hadley Centre's fully-coupled earth system model that was conducted using the IS92a CO_2 emission scenario (Cox *et al.*, 2004). Based on our resulting sensitivity-response matrix (Fig. 2a,b; 8 °C warming and 40% reduction in rainfall), LPJ simulations indicate that C_V and C_S should decrease by approximately 43% and 50%, respectively.

There are two primary differences between the two models used in the example above: (1) LPJ simulations were not conducted under elevated atmospheric CO_2, and (2) LPJ is not a fully coupled model and therefore does not incorporate vegetation feedbacks on climate. Both of these factors could account for the increased reduction in terrestrial carbon storage observed in LPJ simulations, indicating that both the rise in atmospheric CO_2 and vegetation–climate coupling promote resiliency in Amazonian forest to changes in carbon process dynamics.

Does atmospheric CO_2 variation influence threshold responses?

Atmospheric CO_2 does not seem to influence temperature threshold responses in NPP (Fig. 3). Simulated NPP thresholds remain near control temperatures under both ± 100 p.p.m.v. CO_2 scenarios. Atmospheric CO_2 does, however, change the initial value for NPP under control conditions: from 968 to 1032 g C m^{-2} $year^{-1}$ with +100 p.p.m.v. CO_2, and from 968 to 891 g C m^{-2} $year^{-1}$ with −100 p.p.m.v. CO_2. In other words, atmospheric CO_2 shifts the response curve above or below the control curve, but does not influence its overall shape. This response is indicative of an additive (as opposed to multiplicative) environmental stress, supported by various field studies (Cao *et al.*, 2004; Chambers *et al.*, 2004a).

Increases and decreases in atmospheric CO_2 relative to the control do not modify the shape of environmental response curves for vegetation and soil carbon storage, however, once again, the starting and ending points of the curves are influenced by atmospheric CO_2 concentration (Fig. 4). Under high temperature stress (+3 °C to +6 °C), C_V is strongly modified by CO_2 (Fig. 4a), whereas under precipitation stress (−60% to −80%

© 2006 The Authors

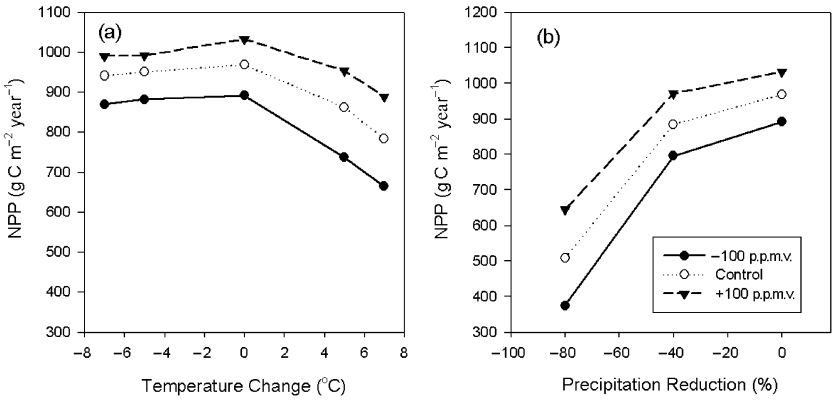

Figure 3 Response of net primary production (NPP) to changes in atmospheric CO_2 (−100 p.p.m.v., +100 p.p.m.v.) in combination with (a) temperature (°C) anomalies, and (b) precipitation reductions (percentage relative to control).

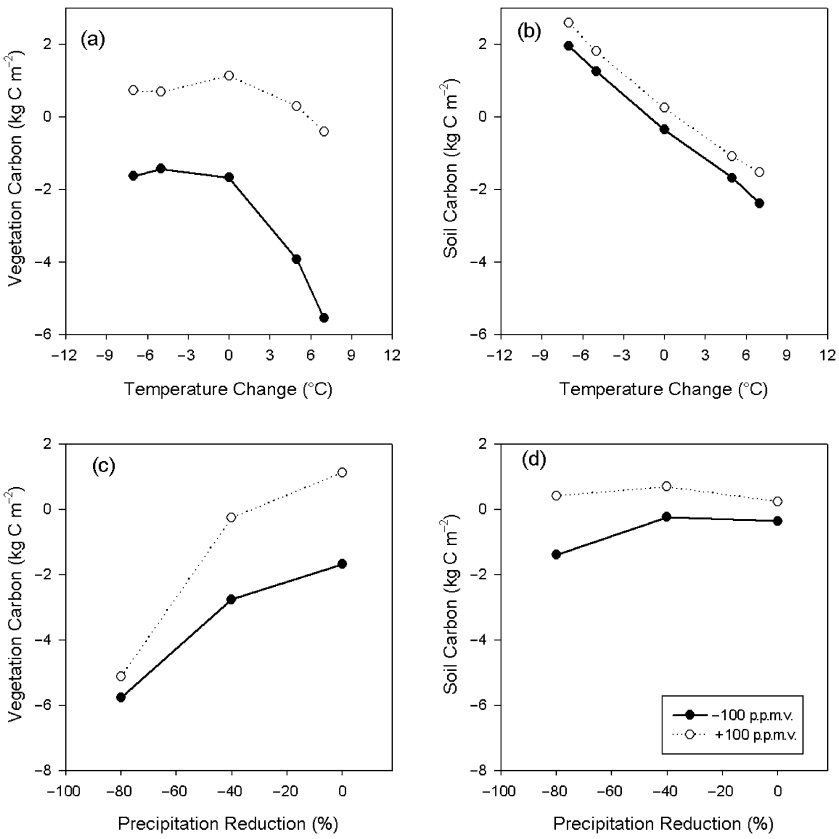

Figure 4 Influence of changes in atmospheric CO_2 (−100 p.p.m.v., +100 p.p.m.v.) on (a) vegetation carbon (C_V) with co-varying temperature anomalies, (b) soil carbon (C_S) with co-varying temperature anomalies, (c) C_V with co-varying precipitation reductions (relative to control), and (d) C_S with co-varying precipitation reductions (relative to control).

reduction), C_V is only minimally influenced by CO_2 (Fig. 4c). Of vegetation and soil carbon responses to co-varying environmental changes in general, CO_2 has the least effect on C_S relative to C_V.

Community-level thresholds and ecosystem resilience assessed through PFT competition

To model PFT composition in any particular region, LPJ follows a set of bioclimatic competition rules, meaning that each PFT is parameterized with climate constraints on growth and establishment (Table 1). Photosynthetic measurements taken from temperate and tropical tree species indicate that temperate trees do in fact have lower temperature growth requirements than tropical PFTs (Cunningham & Read, 2002), supporting assigned differences in PFT growth potential. Once the bioclimatic criteria of a PFT are met, PFTs must then compete for light (which is based on accumulation of carbon). Those that grow the best, establish at a greater rate. There are some static competition rules, such as if both tree and grass PFTs can grow in an area, trees will always out-compete grass. In fact, grass PFTs are usually assigned coverage based on the area of grid cell that is not covered by tree PFTs (Sitch *et al.*, 2003). These 'rules' are not necessarily limitations to PFT-based vegetation modelling research, but rather caveats to keep in mind when analysing modelling results.

Our simulated region contains more than one PFT, although by far the most dominant type is tropical evergreen forest. For our control, fractional coverage by tropical evergreen ('rain forest'), tropical raingreen ('seasonal forest'), temperate woody

© 2006 The Authors

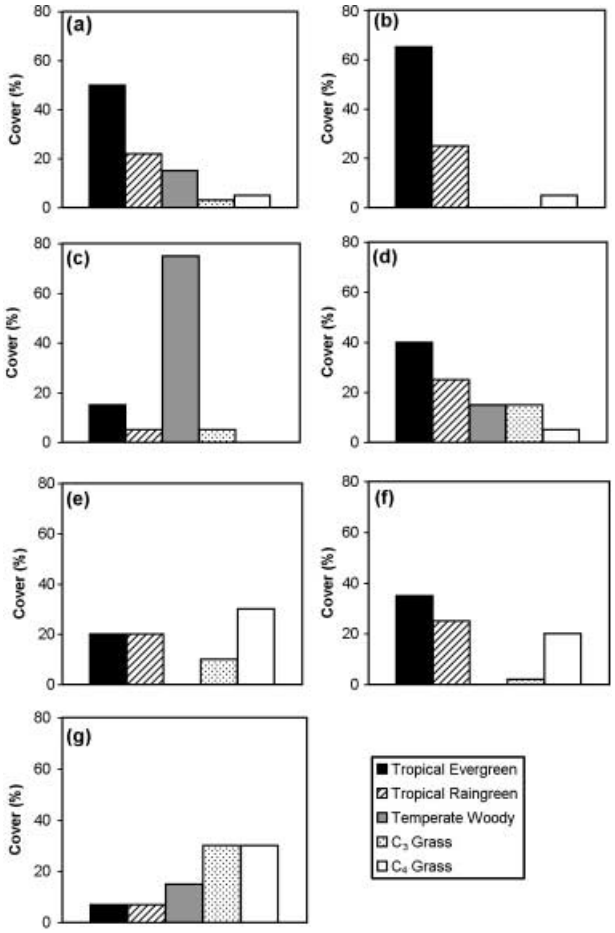

Figure 5 Percentage cover of Amazonian plant functional types (PFTs) under (a) control climate, (b) 7 °C warming, (c) 7 °C cooling, (d) 60% reduction in precipitation relative to control, (e) 80% reduction in precipitation relative to control, (f) 80% reduction in precipitation, combined with 7 °C warming, and (g) 80% precipitation reduction, combined with 7 °C cooling.

plants, C_3 grass, and C_4 grass are 50%, 25%, 15%, 3% and 5%, respectively (Fig. 5a). When we impose climate warming of +7 °C, percentage cover of tropical evergreen forest actually increases from 50% to 70%, replacing temperate and C_3 grass PFTs (Fig. 5b). Under imposed climate cooling, our simulated region of Amazonia is dominated by the temperate woody PFT with concomitant declines in the fractional coverage of warm-loving PFTs (i.e. raingreen and evergreen forest) (Fig. 5c).

Surprisingly, a 60% reduction in precipitation relative to the control does not cause major changes in PFT abundance, although fractional cover by tropical woody types undergoes a slight decline (Fig. 5d). The only simulation that results in significant changes in PFT abundance include those with a reduction in precipitation of up to 80% relative to the control (Fig. 5e), although as indicated earlier (i.e. water stress effects on carbon-based processes), LPJ may result in simulations indicating a precipitation threshold that is far too (unrealistically) tolerant to drought.

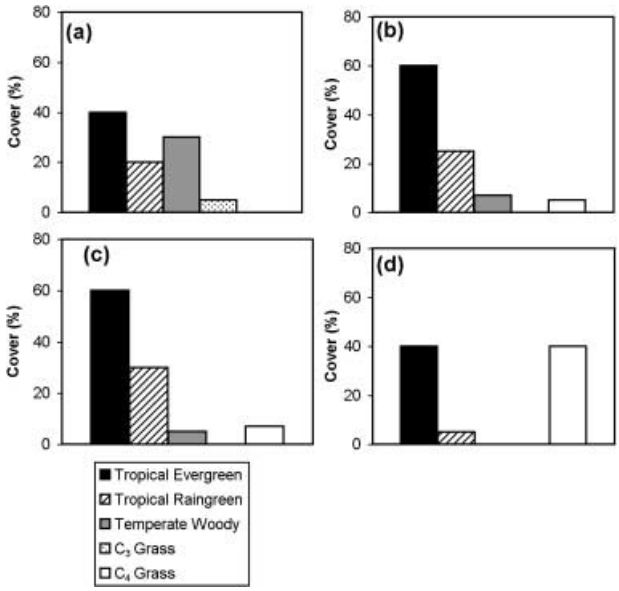

Figure 6 Response of Amazonian plant functional type (PFT) assemblages to (a) high (+100 p.p.m.v.) atmospheric CO_2, (b) low (−100 p.p.m.v.) atmospheric CO_2, (c) high CO_2 in combination with a 40% reduction in control precipitation and 7 °C warming, and (d) low CO_2 in combination with 40% reduction in control precipitation and 7 °C warming.

Under a general reduction in precipitation, the fractional coverage of tropical woody PFTs declines with a corresponding increase in grassy PFTs. Depending on whether the decline in precipitation is accompanied by an increase or decrease in temperature, either C_4 grasses dominate (Fig. 5f) or C_3 and C_4 grasses co-dominate (Fig. 5g), respectively. Reductions in precipitation in combination with climate cooling promote a lower woody PFT percentage cover relative to grassy PFTs, a result that has implications for the behaviour of the Amazon forest during the last glacial maximum (LGM, 21 thousand years ago). Most observational palaeodata and palaeovegetation simulation modelling indicate that although woody cover declined, grass did not dominate Amazonia during the last deglaciation (see references in Cowling *et al.*, 2004). Our simulations indicate that is was the degree of rainfall reductions (and not the degree of temperature cooling) that primarily controlled the balance of tree vs. grass PFT cover in the Amazon. Moreover, even for the highest estimates of drought proposed for glacial Amazonia (60% rainfall decrease), simulations do not indicate a change to extensive grass cover.

Independent decreases (−100 p.p.m.v.) or increases (+100 p.p.m.v.) in atmospheric CO_2 do not result in substantial changes to the PFT assemblage, except that when CO_2 is increased, the C_4 grass PFT disappears (Fig. 6a). On the other hand, combined CO_2, precipitation and temperature changes result in noticeable differences in PFT abundance (Fig. 6c,d). Low precipitation combined with climate warming and higher than control CO_2 levels result in a PFT assemblage much like that for the control scenario, except with the disappearance of the C_3 grass PFT (Fig. 6c).

© 2006 The Authors

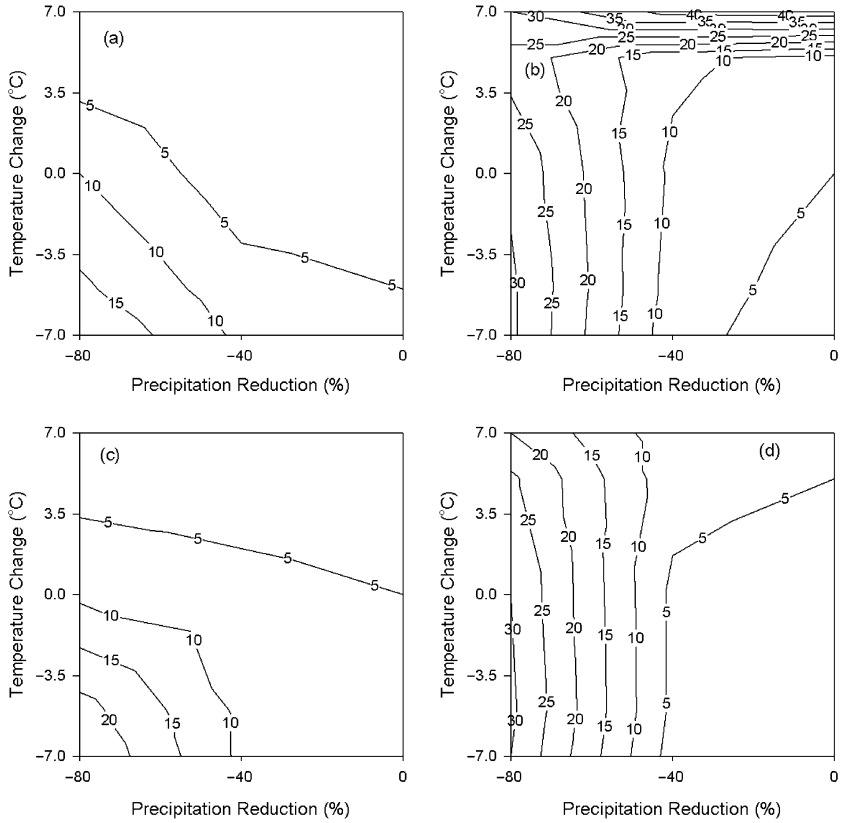

Figure 7 Simulated distributional coverage (%) of (a) C_3 grass under low (−100 p.p.m.v.) atmospheric CO_2, (b) C_4 grass under low (−100 p.p.m.v.) atmospheric CO_2, (c) C_3 grass under high CO_2 (+100 p.p.m.v.), and (d) C_4 grass under high CO_2 (+100 p.p.m.v.), all of which are combined with a range of temperature and precipitation anomalies.

Differences in the simulated percentage cover of C_3 and C_4 grasses across Amazonia can be assessed in terms of the degree of aridity (i.e. decreased precipitation) in combination with climate warming and low CO_2. The distributional pattern of C_3 grass cover within our modelled region of Amazonia does not vary substantially under either low or high CO_2 (Fig. 7a,c). On the other hand, the regional distribution of C_4 grass cover differs depending on the atmospheric CO_2 anomaly (Fig. 7b,d). When CO_2 is lower than control values, the dominant factor controlling C_4 distribution is temperature (Huang *et al.*, 2001). A very strong thermal response threshold for high C_4 plant cover occurs with temperature increases in the range of 4–5 °C (Fig. 7b). These results offer interesting insights for a better understanding of the environmental conditions that led towards the widespread proliferation of C_4 plants during the late-Miocene (7–9 million years ago).

Two variables have been cited as primary catalysts responsible for the near globally synchronous proliferation of C_4 plants during the late-Miocene: increased atmospheric aridity (i.e. drought) and low atmospheric CO_2 (Keeley & Rundel, 2003). A third factor, increasing temperature, is generally given less priority (Cowling, 1999). Our simulations indicate that replicating an abrupt rise in C_4 grass cover requires a sharp 4–5 °C rise in temperature in combination with lower than present CO_2 levels. Generally, increased CO_2 concentrations in the atmosphere lead to increased temperatures (i.e. atmospheric CO_2 and temperature are climatically coupled); however, our scenario requires a brief (rapid) uncoupling of CO_2 and temperature climate trends (i.e. temperatures must increase even though concentration of the greenhouse gas, CO_2, is low). Such a rapid warming mechanism is possible and has been documented for earlier geological periods (the Palaeocene–Eocene boundary). The release of gas hydrates (methane) from the ocean floor can diffuse and be released into the atmosphere, where it can remain as methane (an even stronger greenhouse gas than CO_2) or become oxidized to CO_2.

Although our paper focuses on equilibrium responses and not on transient responses over the 98 years (1901–98) of control climate simulations, we observed a very interesting relationship between low CO_2 and the stabilization of PFT assemblages (data not shown). For most of our modelled climate change scenarios, PFT composition reached equilibrium between 30 and 50 years after the completion of our spin-up simulations. The only exceptions include climate change scenarios involving lower than ambient (−100 p.p.m.v.) atmospheric CO_2.

Low CO_2 combined with 5 °C warming relative to the control results in PFT-equilibrium occurring later, after 70 years of simulation, and yields an ecosystem make-up of 80% fractional coverage by tropical evergreen and 10% by C_4 grass. If we increase climate warming by just an additional 2 °C (i.e. +7 °C relative to the control), the system does not ever reach a true equilibrium, even at the final year of simulation. For this scenario, ecosystem composition shows a dynamic transition between 40% tropical evergreen and 40% C_4 grass. It must be determined whether low atmospheric CO_2 acts to impede equilibrium ecosystem responses to environmental change, or has occurred in our simulations simply as the result of model parameterization. Further study is obviously warranted.

© 2006 The Authors

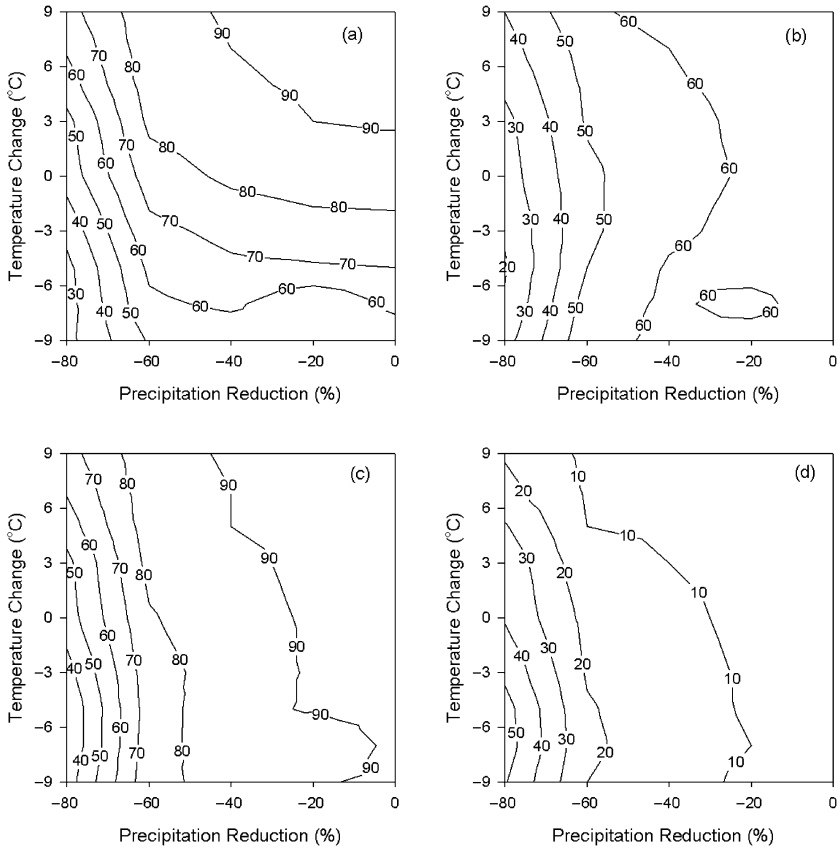

Figure 8 Aggregated plant functional type (PFT) cover (%) simulated in response to temperature and precipitation anomalies in (a) broad-leaved trees, (b) evergreen trees, (c) total tree and (d) total grass.

In general, however, simulated Amazonian ecosystem structure, in terms of aggregated broad-leaved and evergreen PFT cover, exhibits fairly low variability to changes in climate conditions (Fig. 8a,b), thereby demonstrating a type of ecological resilience (*ecological inertia*) to external environmental stimuli. Levi *et al.* (2004) also found this to occur in their Amazonian climate simulations, with relatively low variability in PFT assemblages occurring regardless of whether the ecosystem gained or lost carbon as a whole. Supporting modelling results from Gerber *et al.* (2004) indicate that tropical woody tree coverage can increase with climate warming, even when ecosystem carbon is steadily decreasing. Unfortunately, there is no way for us to test our theory of ecosystem resilience to environmental change in the Amazon Basin (no such large-scale, long temporal experiment exists). What has become apparent through modern-day empirical research is that with anthropogenic disturbance of natural systems, potential inherent resilience in tropical systems is disrupted (Larsen *et al.*, 2005).

CONCLUSIONS

Our covarying sensitivity modelling experiments generally indicate that ecophysiological processes underlying tropical forest dynamics display threshold effects that are not heightened by interactive stresses involving temperature, precipitation and atmospheric CO_2 concentration. In fact, the combination of multiple environmental stresses results in a lessening of the slope of process response curves, making it less obvious, for example, to locate where NPP and R_H thresholds lie. Both NPP and R_H have a simulated temperature threshold near modern-day values, above which both variables decrease with additional warming. This result should raise awareness, particularly in those who believe tropical forests are large sinks for carbon, and that they are likely to remain that way for some time to come.

Our model-predicted precipitation threshold for NPP at 80% reduction in rainfall (relative to the control) is most likely the result of model limitations; LPJ does not incorporate dynamic vegetation feedbacks on climate, nor does it contain refined PFT parameterizations. Atmospheric CO_2 has the least influence on soil carbon storage, even when combined with temperature and precipitation stress. Simulations evaluating ecosystem thresholds (i.e. based on PFT composition/competition) indicate that our modelled region of Amazonia is surprisingly very resilient to change. High temperature stress has minimal influence on simulated PFT assemblages, as does precipitation declines in the order of up to 60% decrease in rainfall, relative to the control.

In the light of our current study, we recommend the following agendas for future research. (1) Investigate why low atmospheric CO_2 (−150 p.p.m.v.) promotes an increase in time taken to reach PFT equilibrium. Our LPJ simulations indicate a potential role for low CO_2 in maintaining ecological inertia, although it must be determined first whether this response is a modelling artefact due to parameterizations or not. (2) Intermediate-complexity (fully-coupled) GCMs should be used to determine ecosystem

© 2006 The Authors

thresholds, particularly with respect to the maintenance of PFT composition, and with respect to temperate vs. tropical vegetation. LPJ simulates little variability in PFT composition with covarying environmental stresses, yet NPP, C_V and C_S are simulated to change in response to abiotic stresses. It may be that PFT stability is hard-wired into models and therefore is unrealistically predicted to be resilient to changes in climate and CO_2. (3) Make better use of the ecophysiological data available for refining definitions of model-based PFTs and refining parameterization of PFT tolerance to environmental stress. Although the use of PFTs in vegetation models was initially a necessity to reduce computational time, their existence within natural ecosystems is based on sound ecological and physiological theory.

ACKNOWLEDGEMENTS

S.A.C. acknowledges that this research was funded in part by the National Sciences and Engineering Research Council of Canada, supplemented by a Connaught New Faculty Matching Grant from the University of Toronto.

REFERENCES

Alcock, J. (2003) Positive feedback and system resilience from graphical and finite-difference models: The Amazon ecosystem — an example. *Earth Interactions*, **7**, paper 5.

Barlow, J. & Peres, C.A. (2004) Ecological responses to El Niño-induced surface fires in central Brazilian Amazonia: management implications for flammable tropical forests. *Philosophical Transactions of the Royal Society of London Series B, Biological Sciences*, **359**, 367–380.

Betts, R.A., Cox, P.M., Collins, M., Harris, P.P., Huntingford, C. & Jones, C.D. (2004) The role of ecosystem–atmosphere interactions in simulated Amazonian precipitation decrease and forest dieback under global climate warming. *Theoretical and Applied Climatology*, **78**, 157–175.

Botta, A., Ramankutty, N. & Foley, J.A. (2002) Long-term variations of climate and carbon fluxes over the Amazon Basin. *Geophysical Research Letters*, **29**, 1319. doi: 10.1029/2001GL013607.

Cao, M., Prince, C.D., Small, J. & Goetz, S.J. (2004) Remotely-sensed inter-annual variations and trends in terrestrial net primary productivity: 1981–2000. *Ecosystems*, **7**, 233–242.

Chambers, J.Q. & Silver, W. (2004a) Some aspects of ecophysiological and biogeochemical responses of tropical forests to atmospheric change. *Philosophical Transactions of the Royal Society of London Series B, Biological Sciences*, **359**, 463–476.

Chambers, J.Q., Tribuzy, E.S., Toledo, L.C., Crispim, B.F., Higuchi, N., dos Santos, J., Araújo, A.C., Kruijt, B., Nobre, A.D. & Trumbore, S.E. (2004b) Respiration from a tropical forest ecosystem: partitioning of sources and low carbon efficiency. *Ecological Applications*, **14**, S72–S88.

Cowling, S.A. (1999) Plants and temperature — CO_2 uncoupling. *Science*, **285**, 1500–1501.

Cowling, S.A., Cox, P.M., Betts, R.A., Ettwein, V.J., Johnes, C.D., Maslin, M.A. & Spall, S.A. (2004) Contrasting simulated past and future responses of the Amazon forest to atmospheric change. *Philosophical Transactions of the Royal Society of London Series B, Biological Sciences*, **359**, 539–547.

Cox, P.M., Betts, R.A., Collins, M., Harris, P.P., Huntingford, C. & Jones, C.D. (2004) Amazonian forest dieback under climate-carbon cycle projections for the 21st century. *Theoretical and Applied Climatology*, **78**, 137–156.

Cramer, W., Bondeau, A., Schaphoff, S., Lucht, W., Smith, B. & Sitch, S. (2004) Tropical forests and the global carbon cycle: impacts of atmospheric carbon dioxide, climate change, and rate of deforestation. *Philosophical Transactions of the Royal Society of London Series B, Biological Sciences*, **359**, 331–343.

Cunningham, S.C. & Read, J. (2002) Comparison of temperate and tropical rainforest tree species: photosynthetic responses to growth temperature. *Oecologia*, **133**, 112–119.

Dargaville, R.J., Heimann, M., McGuire, A.D., Prentice, I.C., Kicklighter, D.W., Joos, F., Clein, J.S., Esser, G., Foley, J., Kaplan, J., Meier, R.A., Melillo, J.M., Moore,B., III Ramankutty, N., Reichenan, T., Schloss, A., Sitch, S., Tian, H., Williams, L.J. & Wittenberg, U. (2002) Evaluation of terrestrial carbon cycle models with atmospheric CO_2 measurements: results from transient simulations considering increasing CO_2, climate, and land-use effects. *Global Biogeochemical Cycles*, **16** (4), 1092. doi: 10.1029/2001GB001426.

DeFries, R.S., Townsend, J.R.G. & Hansen, M.C. (1999) Continuous fields of vegetation characteristics at the global scale at 1-km resolution. *Journal of Geophysical Research*, **104**, 16911–16925.

DeFries, R.S., Hansen, M.C., Townsend, J.R.G., Janetos, A.C. & Loveland, T.R. (2000) A new global 1-km dataset of percentage tree cover derived from remote sensing. *Global Change Biology*, **6**, 247–254.

Eiswerth, M.E. & Haney, J.C. (2001) Maximizing conserved biodiversity: why ecosystem indicators and thresholds matter. *Ecological Economics*, **38**, 259–274.

Foley, J.A., Botta, A. & Coe, M.T. (2002) El Niño-Southern Oscillation and the climate, ecosystems and rivers of Amazonia. *Global Biogeochemical Cycles*, **16**, doi: 10.1029/2002GB001872.

García-Romero, A., Oropeza-Orozco, O. & Galicia-Sarmiento, L. (2004) Land-use systems and resilience of tropical rain forests in the Tehuantepec Isthmus, Mexico. *Environmental Management*, **34**, 768–785.

Gerber, S., Joos, F. & Prentice, I.C. (2004) Sensitivity of a dynamic global vegetation model to climate and atmospheric CO_2. *Global Change Biology*, **10**, 1223–1239.

Gordon, W.S., Famiglletti, J.S., Fowler, N.L., Kittel, T.G.F. & Hubbard, K.A. (2004) Validation of simulated runoff from six terrestrial ecosystem models: results from VEMAP. *Ecological Applications*, **14**, 527–545.

Haxeltine, A. & Prentice, I.C. (1996) BIOME3: an equilibrium terrestrial biosphere model based on ecophysiological constraints, resource availability, and competition among plant functional types. *Global Biogeochemical Cycles*, **10**, 693–709.

House, J.I., Prentice, I.C., Ramankutty, N., Houghton, R.A. & Heimann, M. (2003) Reconciling apparent inconsistencies in

© 2006 The Authors

estimates of terrestrial CO_2 sources and sinks. *Tellus B*, **55**, 345–363.

Huang, Y., Street-Perrott, F.A., Melcalfe, S.E., Brenner, M., Moreland, M. & Freeman, K.H. (2001) Climate change as the dominant control on glacial-interglacial variations in C_3 and C_4 plant abundance. *Science*, **293**, 1647–1651.

Joos, F., Gerber, S., Prentice, I.C., Otto-Bliesner, B.L. & Valdes, P.J. (2004) Transient simulations of Holocene atmospheric carbon dioxide and terrestrial carbon storage since the Last Glacial Maximum. *Global Biogeochemical Cycles*, **18**, doi: 10.1029/2003GB002156.

Kaplan, J.O., Prentice, I.C., Knorr, W. & Valdes, P.J. (2002) Modeling the dynamics of terrestrial carbon storage since the Last Glacial Maximum. *Geophysical Research Letters*, **29** (22), doi: 10.1029/2002GL015230.

Keeley, J.E. & Rundel, P.W. (2003) Evolution of CAM and C-4 carbon-concentrating mechanisms. *International Journal of Plant Sciences*, **164**, S55–S77.

Kicklighter, D.W., Bruno, M., Donges, S., Esser, G., Heimann, M., Helfrich, J., Ift, F., Joos, F., Kaduk, J., Kohlmaier, G.H., McGuire, A.D., Melillo, J.M., Meyer, R., Moor, B., Nadler, A., Prentice, I.C., Sauf, W., Schloss, A.L., Sitch, S., Wittenberg, U. & Wurth, G. (1999) A first-order analysis of the potential role of CO_2 fertilization to affect the global carbon budget: a comparison of four terrestrial biosphere models. *Tellus B*, **51**, 343–366.

Kucharik, C.J., Foley, J.A., Delire, C., Fisher, V.A., Coe, M.T., Lenters, J.D., Young-Molling, C., Ramankutty, N., Norman, J.M. & Gower, S.T. (2000) Testing the performance of a dynamic global ecosystem model: water balance, carbon balance, and vegetation structure. *Global Biogeochemical Cycles*, **14**, 795–825.

Larsen, T.H., Williams, N.M. & Kremen, C. (2005) Extinction order and altered community structure rapidly disrupt ecosystem functioning. *Ecology Letters*, **8**, 538–547.

Laurance, W.F. (2003) Slow burn: the insidious effects of surface fires on tropical forests. *Trends in Ecology & Evolution*, **18**, 209–212.

Laurance, W.F. & Williamson, G.B. (2001) Positive feedbacks among forest fragmentation, drought, and climate change. *Conservation Biology*, **15**, 1529–1535.

Levi, P.E., Cannell, M.G.R. & Friend, A.D. (2004) Modeling the impact of future changes in climate, CO_2 concentration and land use on natural ecosystems and the terrestrial carbon sink. *Global Environmental Change*, **14**, 21–30.

Lindenmayer, D.B., Fischer, J. & Cunningham, R.B. (2005) Native vegetation cover thresholds associated with species responses. *Biological Conservation*, **124**, 311–316.

Lucht, W., Prentice, I.C., Myneni, R.B., Sitch, S., Friedlingstein, P., Cramer, W., Bousquet, P., Buermann, W. & Smith, B. (2002) Climatic control of the high-latitude vegetation greening trend and Pinatubo effect. *Science*, **296**, 1687–1689.

Malhi, Y., Baker, T.R., Phillips, O.L., Almeida, S., Alvarez, E., Arroyo, L., Chave, J., Czimczik, C.I., Di Fiore, A., Higuchi, N., Killeen, T.J., Laurance, S.G., Laurance, W.F., Lewis, S.L., Montoya, L.M.M., Monteagudo, A., Neil, D.A., Vargas, P.N., Paino, S., Pitman, N.C.A., Quesada, C.A., Salomao, R., Silva, J.N.M., Lezama, A.T., Martines, R.V., Terborgh, J., Vincet, B. & Lloyd, J. (2004) The above-ground coarse wood productivity of 104 neotropical forest plots. *Global Change Biology*, **10**, 563–591.

Marengo, J.A., Miller, J.R., Russell, G.L., Rosenzweig, C.E. & Abramopoulos, F. (1994) Calculations of river-runoff in the GISS GCM: impact of a new land-surface parameterization and runoff routing model on the hydrology of the Amazon River. *Climate Dynamics*, **10**, 349–361.

Mayer, A.L. & Rietkerk, M. (2004) The dynamic regime concept for ecosystem management and restoration. *Bioscience*, **54**, 1013–1020.

McGuire, A.D., Sitch, S., Clein, J.S., Sitch, S., Clein, J.S., Dargaville, R., Esser, G., Foley, J., Heimann, M., Joos, F., Kaplan, J., Kicklighter, D.W., Meier, R.A., Melillo, J.H., Moore, B., Prentice, I.C., Ramankutty, N., Reichenau, T., Schloss, A., Tian, H., Williams, L.J. & Wittenberg, U. (2001) Carbon balance of the terrestrial biosphere in the twentieth century: analyses of CO_2, climate and land use effects with four process-based ecosystem models. *Global Biogeochemical Cycles*, **15**, 183–206.

New, M., Hulme, M. & Jones, P.D. (2000) Representing twentieth-century space-time climate variability. Part II: Development of 1901–96 monthly grids of terrestrial surface climate. *Journal of Climate*, **13**, 2217–2238.

New, M., Hulme, M. & Jones, P.D. (2003) LBA regional monthly climatology for the 20th century. Dataset on-line at http://www.daac.ornl.gov from Oak Ridge National Laboratory Distributed Active Archive Center, Oak Ridge, Tennessee, USA.

Olson, J.S., Watts, J.A. & Allison, L.J. (2003) *Major world ecosystem complexes ranked by carbon in live vegetation.* Dataset on-line at http://www.daac.ornl.gov from Oak Ridge National Laboratory Distributed Active Archive Center, Oak Ridge, Tennessee, USA.

Peterson, G., Allen, C.R. & Holling, C.S. (1998) Ecological resilience, biodiversity and scale. *Ecosystems*, **1**, 6–18.

Peylin, P., Bousquet, P., LeQuere, C., Sitch, S., Friedlingstein, P., McKinley, G., Gruber, N., Rayner, P. & Cias, P. (2005) Multiple constraints on regional CO_2 flux variations over land and oceans. *Global Biogeochemical Cycles*, **19**, GB1011, doi: 10.1029/2003GB002214

Phillips, O.L., Malhi, Y., Higuchi, N., Laurance, W.F., Nunes, D.V., Vasquez, R.M., Laurance, S.G., Ferreira, L.V., Stern, M., Brown, S. & Grace, J. (1998) Changes in the carbon balance of tropical forests: evidence from long-term plots. *Science*, **282**, 439–442.

Post, W.M., King, A.W. & Wullschleger, S.D. (1997) Historical variations in terrestrial biospheric carbon storage. *Global Biogeochemical Cycles*, **11**, 99–109.

Post, W.M. & Zobler, L. (2000) Global soil types, 0.5-degree grid (Modified Zobler). Dataset available online at http://www.daac.ornl.gov from Oak Ridge National Laboratory Distributed Active Archive Center, Oak Ridge, Tennessee.

Potter, C., Klooster, S., de Carvalho, C.R., Genovese, V.B., Torregrosa, A., Dungan, J., Bobo, M. & Coughlan, J. (2001) Modeling seasonal and inter-annual variability in ecosystem

© 2006 The Authors

carbon cycling for the Brazilian Amazon region. *Journal of Geophysical Research*, **106** (D10), 423–410.

Potter, C., Klooster, S., Steinbach, M., Tan, P., Kumar, V., Shekhar, S. & de Carvalho, C.R. (2004) Understanding global teleconnections of climate to regional model estimates of Amazon ecosystem carbon fluxes. *Global Change Biology*, **10**, 693–703.

Prentice, I.C., Farquhar, G.D., Fasham, M.J.R., Goulden, M.L., Heimann, M., Jaramillo, V.J., Kheshgi, H.S., Le Quere, C., Scholes, R.J. & Wallace, D.W.R. (2001) The carbon cycle and atmospheric carbon dioxide. *Climate change 2001: the scientific basis* (ed. by J.T. Houghton, D.J. Griggs, M. Noguer, P.J. Van Der Linden, X. Dai, K. Maskell and C. A. Johnson), pp. 184–237. Cambridge University Press, Cambridge.

Radford, J.Q., Bennett, A.F. & Cheers, G.J. (2005) Landscape-level thresholds of habitat cover for woodland-dependent birds. *Biological Conservation*, **124**, 317–337.

Raich, J.W. & Schlesinger, W.H. (1992) The global carbon dioxide flux in soil respiration and its relationship to vegetation and climate. *Tellus B*, **44**, 81–99.

Raich, J.W., Potter, C.S. & Bhagawati, D. (2002) Inter-annual variability in global soil respiration: 1980–94. *Global Change Biology*, **8**, 800–812.

Ramankutty, N. & Foley, J.A. (1999) Estimating historical changes in global land cover: croplands from 1700 to 1992. *Global Biogeochemical Cycles*, **13**, 997–1027.

Reynolds, C.S. (2002) Ecological pattern and ecosystem theory. *Ecological Modelling*, **158**, 181–200.

da Rocha, H.R., Nobre, C.A., Bonatti, J.P., Wright, I.R. & Sellers, P.J. (1996) A vegetation–atmosphere interaction study for Amazonian deforestation using field data and a 'single column' model. *Quarterly Journal of the Royal Meteorological Society*, **122**, 567–594.

Silver, W.L. (1998) The potential effects of elevated CO_2 and climate change on tropical forests soils and biogeochemical cycling. *Climatic Change*, **39**, 337–361.

Sitch, S., Smith, B., Prentice, I.C., Arneth, A., Bondeau, A., Cramer, W., Kaplan, J.O., Levis, S., Lucht, W., Sykes, M.T., Thonicke, K. & Venevsky, S. (2003) Evaluation of ecosystem dynamics, plant geography and terrestrial carbon cycling in the LPJ dynamic global vegetation model. *Global Change Biology*, **9**, 161–185.

Sitch, S., Brovkin, V., von Bloh, W., van Vuuren, D., Assessment, B. & Ganopolski, A. (2005) Impacts of future land cover changes on atmospheric CO_2 and climate. *Global Biogeochemical Cycles*, **19**, GB2013, doi: 10.1046/j.1365-2486.2003.00569.x

Smith, B., Prentice, I.C. & Sykes, M.T. (2001) Representation of vegetation dynamics in the modelling of terrestrial ecosystems: comparing two contrasting approaches within European climate space. *Global Ecology and Biogeography*, **10**, 621–637.

Stringham, T.K., Krueger, W.C. & Shaver, P.L. (2003) State and transition modeling: an ecological process approach. *Journal of Range Management*, **56**, 106–113.

Tian, H., Melillo, J.M., Kicklighter, D.W., McGuire, A.D., Helfrich III, J., Moore III, B. & Vorosmarty, C.J. (2000) Climatic and biotic controls on annual carbon storage in Amazonian ecosystems. *Global Ecology and Biogeography*, **9**, 315–335.

Townsend, A.R. & Vitousek, P.M. (1992) Carbon cycle feedbacks to increased global temperature. *Climatic Change*, **22**, 293–303.

With, K.A., Pavuk, D.M., Worchuck, J.L., Oates, R.K. & Fisher, J.L. (2002) Threshold effects of landscape structure on biological control in agro-ecosystems. *Ecological Applications*, **12**, 52–65.

Yuste, J.C., Janssens, I.A., Carrara, A., Meiresonne, L. & Ceulemans, R. (2003) Interactive effects of temperature and precipitation on soil respiration in a temperate maritime pine forest. *Tree Physiology*, **23**, 1263–1270.

Zinke, P.J., Strangenberger, A.J., Post, W.M. & Olson, J.S. (2003) *LBA regional organic soil carbon and nitrogen data (Zinke et al.).* Dataset available online at http://www.daac.ornl.gov from Oak Ridge National Laboratory Distributed Active Archive Center, Oak Ridge, Tennessee, USA.

BIOSKETCHES

Sharon Cowling is an assistant professor in Earth Systems at the Department of Geography, University of Toronto. She has been interested in modelling vegetation–climate interactions in the Amazon Basin since her PhD, and intends to couple this interest with field-based research approaches.

Younglan Shin is a research assistant in Sharon Cowling's laboratory. She assists with ongoing modelling applications and has conducted original research on the simplification of C_3/C_4 photosynthetic models. She intends to produce a coupled atmosphere–biosphere model for use during her upcoming PhD graduate research.

Editor: Martin Sykes

© 2006 The Authors